Efficient conversion of lignin into a water-soluble polymer by a chelator-mediated Fenton reaction: optimization of H2O2 use and performance as a dispersant

Journal:	*Green Chemistry*
Manuscript ID	GC-ART-11-2017-003459.R1
Article Type:	Paper
Date Submitted by the Author:	15-Apr-2018
Complete List of Authors:	Kent, Michael; Sandia National Laboratories, Biological and Materials Sciences Center; Joint BioEnergy Institute Zeng, Jijao; Sandia National Laboratories California; Joint BioEnergy Institute; Key Laboratory of Green Catalysis of Higher Education Institutes of Sichuan, Sichuan University of Science & Engineering, College of Chemistry and Environmental Engineering Rader, Nadeya; Sandia National Laboratories, Biological and Materials Sciences Center Avina, Isaac; Sandia National Laboratories, Biological and Materials Sciences Center Simoes, Casey; Sandia National Laboratories, Biological and Materials Sciences Center Brenden, Christopher; Sandia National Labs, Biological and Materials Sciences Center Busse, Michael; Sandia National Laboratories, Biological and Materials Sciences Center Watt, John; Sandia National Laboratories, Center for Integrated Nanotechnologies Giron, Nicholas; Sandia National Laboratories, Biological and Materials Sciences Center Alam, Todd; Sandia National Laboratory, Electronic and Nanostructured Materials Allendorf, Mark; Sandia National Laboratory, Simmons, Blake; E O Lawrence Berkeley National Laboratory, Biological Systems and Engineering; Joint BioEnergy Institute Bell, Nelson; Sandia National Laboratories, Electronic & Nanostructured Materials Sale, Kenneth; Joint BioEnergy Institute, Enzyme Optimization Group; Sandia National Laboratories, Biomass Science and Conversion Technology

Green Chemistry

PAPER

Efficient conversion of lignin into a water-soluble polymer by a chelator-mediated Fenton reaction: optimization of H_2O_2 use and performance as a dispersant

Michael S. Kent,[†,§,*] Jijiao Zeng,[†,§] Nadeya Rader,[§] Isaac C. Avina,[§] Casey T. Simoes,[§] Christopher K. Brenden,[§] Michael L. Busse,[§] John D. Watt,[§] Nicholas H. Giron,[§] Todd M. Alam,[§] Mark D. Allendorf, Blake A. Simmons,[†,**] Nelson S. Bell[§] and Kenneth L. Sale[†,§]

Room temperature Fenton (FEN) and chelator-mediated Fenton (CMF) reactions were examined for transforming lignin into a water-soluble polymer. Compared to depolymerization of lignin, this has the advantage of potentially yielding a product directly without requiring further upgrading. With the goal of optimizing the use of the expensive reagent H_2O_2, initial studies were performed with lignin from an organsolv process (OS) in thin films with a multi-well format that allows simultaneous assay of 76 reaction conditions. The results showed that H_2O_2 is more efficiently used in CMF compared with FEN, and that the greatest amount of lignin solubilized per mass of H_2O_2 consumed occurs at low initial concentrations of H_2O_2 (< 1%). Further optimization of reaction conditions was performed with OS lignin in powder form. Results obtained upon optimizing reactant concentrations, pH, Fe-chelator, and with O_2 bubbling indicate that a yield of 1 g lignin solubilized per g of H_2O_2 consumed is achievable. Chemical and molecular weight analyses showed that the reaction results in extensive opening of the aromatic rings and generation of acid groups, yielding a water-soluble polymer with molecular weight distribution that is comparable to that of the starting material but with a small amount of low MW species. Similar yields and extents of ring opening resulted for three other distinctly different lignins. The effectiveness of the OS lignin-derived polymeric material in dispersing alumina particles was studied by zeta potential, light scattering, and Turbiscan stability measurements. These measurements showed that the lignin-derived material performs comparably to poly(acrylic acid) PAA of similar molecular weight. Considering that the sellling price for bulk PAA is greater than twice that of H_2O_2 on a per mass basis, this approach holds promise for generating value from lignin.

Received 00th January 20xx,
Accepted 00th January 20xx

DOI: 10.1039/x0xx00000x

www.rsc.org/

1. Introduction

Valorizing lignin has the potential to significantly improve the economics of biomass conversion technologies.(1-4) Lignin comprises 15-30% of the mass of lignocellulosic biomass and is currently burned for its heating value within a biorefinery. Generating greater value out of this carbon has the potential to substantially impact the economic viability of lignocellosic conversion.

Many different approaches for lignin conversion to valuable products are being pursued. Some of these involve depolymerization of lignin followed by upgrading the complex mixture of small molecule products. Biological upgrading is a promising approach for dealing with the complexity of lignin breakdown products.(5-7) While this approach may have great potential for valorizing large amounts of lignin, many difficult hurdles are still to be overcome. Not the least of which is the need to convert the majority of lignin into low molecular weight species that can be taken up by bacteria or fungi and are not toxic.(8) Depolymerization of lignin is an energy intensive process. An alternative in the short term, or perhaps for particularly condensed or intransigent fractions of a lignin stream, is to develop processes that add value to the lignin polymer that nature has already constructed rather than depolymerize it. Production of carbon fibers from lignin is one example of this approach.(9)

In this work we explored the use of the Fenton reaction (FEN) and chelator-mediated Fenton (CMF) reaction to generate a useful material from lignin by directly transforming it into a water-soluble polymer. In these well-studied reactions (10-20) Fe(II) reacts with H_2O_2 to yield Fe(III) and hydroxyl radical, which is a highly potent oxidant. For Fe to be used catalytically, Fe(III) must be reduced to Fe(II). In FEN this occurs slowly, and inefficiently with respect to H_2O_2 usage, through reaction of Fe(III) with H_2O_2. In CMF, reduction of Fe(III) to Fe(II) occurs more rapidly and without consuming H_2O_2 using an organic Fe chelator/reducer. In addition to improved oxidative efficiency, CMF operates efficiently over a wider pH range than FEN, which is only effective near pH 3 (to avoid oxidation of Fe(II) to $Fe(OH)_3$ or Fe_2O_3).(21) We show that under optimal

† *Joint BioEnergy Institute, Emeryville, CA 94608*
§ *Sandia National Laboratories, Livermore, CA and Albuquerque, NM 87185*
** *Lawrence Berkeley National Laboratory, Berkeley CA 94720*
* *To whom correspondence should be addressed: mskent@sandia.gov*
† Footnotes relating to the title and/or authors should appear here.
Electronic Supplementary Information (ESI) available: [details of any supplementary information available should be included here]. See DOI: 10.1039/x0xx00000x

CMF conditions H_2O_2 can be used efficiently to open nearly all the aromatic rings in lignin, yielding acid groups. This is accomplished with very little reduction in molecular weight and with sparing use of H_2O_2. The reaction produces a valuable functionalized material directly from even the most intransigent portion of a lignin stream. While most of our studies involved organosolv (OS) lignin, a comparable extent of aromatic ring opening and comparable yields of water-soluble polyacid were obtained with Kraft Indulin AT (KRAFT), lignin from treatment of switchgrass with the ionic liquid 1-ethyl-3-methylimidazolium acetate (IL), and lignin from corn stover obtained through a process involving deacetylation, mechanical refinement, and enzymatic hydrolysis (DMR-EH). As for other polyacids, such as lignosulfonates and poly(acrylic acid) (PAA), the lignin-derived water-soluble polyacid product has many potential applications, including as a thickener, dispersing agent, emulsifying agent, plasticizer for concrete and cement, curing agent for adhesives, water-reducer in plasterboard/fiberboard, or viscosity reducer of drilling fluid in oil drilling. Furthermore, the polyacid material could be crosslinked to form a hydrogel. As an example of a potential application of this lignin-derived polyacid material we demonstrate that, without further upgrading or separation, the material derived from OS lignin performs comparably to PAA in dispersing alumina particles.

The economic viability of this process requires highly efficient use of the expensive reagent H_2O_2 (~ $400/MT for 50% solution) Prior work involving FEN for biomass conversion has typically involved relatively large amounts of H_2O_2 (> 5%).(22, 23) With the goal of maximizing efficient use of H_2O_2, we performed an initial optimized of CMF reaction conditions using an assay for lignin solubilization based on insoluble lignin films, followed by further optimization using lignin in powder form. In prior work FEN and CMF reactions have been explored extensively for use in water purification.(11, 15-17, 19, 21, 24-28) In that case, the presence of substrate in dilute concentration makes efficient use of H_2O_2 especially challenging since hydroxyl radicals are highly reactive.(19) Our work shows that H_2O_2 is used most efficiently at low H_2O_2 concentration (0.5%) and high substrate concentration.

We demonstrate that the product of the reaction is a ring-opened polymer of comparable molecular weight to the original material but including a small amount of low molecular weight species. Possible uses of a water-soluble polyacid from lignin include, but are not limited to, as a dispersant or as an anti-fouling agent for water handling equipment. PAA, derived from petrochemicals, is an industry standard polymer used in these applications, and therefore we compared the lignin-derived water-soluble polymer to PAA for dispersing alumina particles.

2. Experimental Section

2.1 Materials

Organosolv (OS) lignin was obtained from Lignol Corp. Kraft Lignin Indulin AT was purchased from Aldrich Chemical Co. IL lignin was generated at the Joint BioEnergy Institute using a pretreatment process described previously.(29) DMR-EH lignin (30) was a gift from D. Salvachúa. Aminopropyltriethoxysilane (APS), 2,2'-azino-bis(3-ethylbenzothiazoline-6-sulphonic acid) (ABTS), $FeCl_2$, $FeCl_3$ hexahydrate, 1,2-dihydroxybenzene (DHB), 2,3-dihydroxybenzoic acid (DHBA), 1,2,3 trihydroxybenzene, poly(acrylic acid) with weight average molecular weight of 2000 g/mol, KNO_3, HNO_3, and KOH were purchased from Sigma-Aldrich. H_2O_2 (~ 35%) was purchased from Fisher Scientific. Laccase from *Tinea versicolor* (10 U/mg) was purchased from US Biological. Silicon wafers were undoped type N with 1-0-0 orientation. Alpha alumina oxide powder AKP-30 was obtained from Sumitomo Corp.

2.2 Reactions involving lignin films

Preparation of lignin films for use in this assay has been described previously.(31) Prior to coating the silicon substrates with lignin, APS was deposited to promote adhesion. Silicon wafers (3-inch diameter) were first cleaned with detergent solution and then received UV-ozone treatment for 30 min. Smooth films of APS were deposited onto UV-ozone cleaned silicon wafers by spin coating. APS was dissolved into 90/10 ethanol/water at 0.25 % and stirred for 60 min. The solution was then spin coated onto the silicon wafers at 3000 rpm. Afterwards the APS-coated wafers were heated in vacuum at 70 C for 1 hr to drive off the water and cure the film.

Lignin was dissolved at 3% in 1,4 dioxane, filtered through a 1 μM syringe filter, and spin coated onto silicon wafers using a Headway photo resist spinner model 1-PM101DT-R790 at 1500-4000 rpm. This concentration resulted in final film thicknesses (after treatment with oxidized ABTS described below) ranging from 750 Å-950 Å depending upon spinning speed. This thickness range was optimal for these measurements as film uniformity was compromised for thicker films. The lignin-coated wafers were heated in vacuum at 70 ^{O}C for 1 hr to drive off the dioxane.

The lignin film assay measures the solubilization of lignin upon reaction, and therefore requires a lignin film that is largely insoluble in absence of reaction. In the course of our studies we found that the solubility of OS lignin increases substantially with increasing concentration of H_2O_2 ($[H_2O_2]$). Therefore, to screen over a wide range of $[H_2O_2]$, the lignin films were first treated with oxidized ABTS to reduce the film solubility in the presence of high $[H_2O_2]$. Laccase (25 μg/ml) was added to a 1 mM solution of ABTS in 10 mM sodium lactate buffer at pH 4.5 and allowed to catalyze the oxidation of ABTS for 30 min. UV absorbance indicated that under these conditions the maximum concentration of oxidized ABTS is achieved after incubation for 20 min. Following incubation for 30 min, the solution was filtered through a 10,000 g/mol molecular weight cutoff (MWCO) filter to remove the laccase. The lignin films were then incubated against the solution of oxidized ABTS overnight. The wafers were then removed and rinsed thoroughly with Millipore water.

Film thickness measurements were automated using a NanoSpec 6100 spectral reflectometer from Nanometrics, with a wavelength range of 480 – 800 nm. By means of a motorized sample stage and a pre-defined test pattern, the tool semi-autonomously measured each well location. Pre-reaction data were collected with one measurement per well location. Post-

reaction data were collected in triplicate, with measurement sites targeted at the center of the well, offset slightly above the center line, and offset slightly below the centerline.

2.3 Reactions involving lignin powder

Reactions using lignin powder as the substrate were performed in 20 ml vials with 8 ml of liquid. A stock solution of 10 mM $FeCl_3$ and 10 mM DHB was prepared and the pH adjusted to the desired initial value for the reaction using NaOH. The appropriate amount of this stock solution to achieve the desired concentration was added to the reaction vial along with lignin, and Millipore water (also adjusted to the desired pH). The mixture was stirred with a magnetic stirring bar for 24 h to disperse the lignin and then the appropriate amount of aqueous H_2O_2 was added to initiate the reaction. The reactions were allowed to proceed for 48 h (much longer than necessary) and then the suspensions were centrifuged at 13000 x g for 5 minutes to separate water-soluble material from the insoluble lignin. The water insoluble material was thoroughly dried in a vacuum oven and then weighed to determine the mass of lignin solubilized as the difference from the initial weight. For each reaction a control was included for which no H_2O_2 was added. This was processed in an identical fashion to the reacting samples. For these control samples a few percent mass loss was consistently observed as a small amount of lignin material is soluble in the reaction medium in absence of reaction. The mass loss for the control was subtracted from the mass loss for the reacting samples and the difference was reported as mass solubilized by the reaction. The control measurements indicated whether or not the chelator complex was insoluble or associated strongly with the insoluble lignin. With DHB, the mass of the Fe(DHB) complex was measured with the insoluble pellet whereas for DHBA the mass of the Fe(DHBA) complex remained in solution.

A series of successive reactions were performed to compare with results for single batch reactions. In this case after reaction the liquid and solid were separated by centrifugation, the liquid was decanted, and new aliquots of the reactants and H_2O were added. For each successive reaction the amounts of reactants were added to achieve the same initial concentrations and the total volume was adjusted to achieve the same mass of lignin per volume, accounting for the decreased amount of lignin that resulted from solubilization during the prior reaction.

GPC. The molecular weight distribution of the water-soluble material from reactions with lignin powder was measured using an Agilent 1260 HPLC system with PL Aquagel-OH 30 and PL Aquagel-OH 50 columns in series and UV detection at 210 nm. Because of the amphiphilic nature of the lignin-derived polyacid, special care was taken to avoid or minimize aggregation during the measurement. In a series of measurements it was determined that the water-soluble product material was not fully soluble at high salt concentrations. A sample was measured at a series of decreasing phosphate buffer concentrations until little change was observed in the chromatograms. A 1 mM PO_4 buffer was used for the molecular weight determinations, using polyacrylic acid standards and also methacrylic acid for calibration. The molecular weight distribution of the original LIgnol lignin was measured in THF using an Agilent 1100 series with two Millipore Waters Styragel HR 4E columns. In that case PS standards were used for calibration.

FTIR. FTIR spectra were collected from residual solid material after evaporating reaction liquids onto Teflon substrates and drying the samples in vacuum to remove the solvent. IR spectra were collected with a Bruker LUMOS ATR-FTIR microscope using a germanium probe tip contacting the material of interest. For each sample, a total of 3 spectra were taken and averaged, where each spectrum consisted of 16 averaged scans at a resolution of 4 cm^{-1}. Spectra were referenced to a non-sample background and an atmospheric correction was applied to remove water and CO_2 vapor contributions.

NMR. NMR samples were prepared by dissolving 25 mg of lignin material in DMSO-d_6 (750 ml). These mixtures were alternately sonicated with a 10% duty cycle for 30 min, then thermally in a 50 ^{o}C water bath for complete dissolution. The 1D ^{13}C NMR and 2D ^{1}H-^{13}C heteronuclear single quantum correlation (HSQC) NMR spectra were obtained using a Bruker-Avance III 600 MHz instrument at a sample temperature of 50°C. The single pulse Bloch decay ^{13}C NMR spectra were obtained on a 5 mm broadband probe, ^{1}H decoupling, and a recycle delay of 10 s, but was not optimized for quantitative ^{13}C integration. For the 2D HSQC (Heteronuclear Single Quantum Correlation) a 5 mm inverse-detected probe was used with the Bruker standard pulse program hsqcetgsp.2 which incorporates an echo/anti-echo-TPPI acquisition scheme with gradient selection, and shaped inversion pulses on the ^{13}C channel. Spectral widths were 8000 Hz and 25000 Hz for the ^{1}H-and ^{13}C-dimensions, respectively. Signal averaging of 128 scans were taken in the F2 dimension with 256 t_1 time increments recorded, using a recycle delay of 1.5 s. The ^{1}H and ^{13}C NMR chemical shifts were referenced to the DMSO solvent resonance (δC/δH +39.5/+2.5 ppm) with respect to TMS δ = 0 ppm.

2.4 Testing dispersant properties of the water-soluble product from CMF

Preparation of dispersions for Zeta potential, particle size distribution, and Turbiscan stability analysis. Alpha aluminum oxide, α-Al_2O_3, was used as the ceramic powder for dispersion testing. For zeta potential and particle size distribution measurements, alumina powder, KNO_3 stock solution, aqueous lignin-derived dispersant (or PAA) solution, and water were combined to yield 1-4 mg lignin (or PAA) per gram alumina powder at 10% solids loading. For Turbiscan stability analysis, 8 g alumina powder were mixed with KNO_3 stock solution, aqueous lignin-derived dispersant (or PAA) solution, and water to yield 40 ml of 1 mM KNO_3, 4 mg dispersant / g alumina, and 5 volume % solids. Dispersion was achieved using an ultrasonic probe (Branson ultrasonics) at 50% power for 10 minutes in a cup horn cell to break up weak agglomerates.

Particle size distribution by light scattering. Measurement of particle size was conducted using a Zetasizer Nano-ZS from Malvern instruments. The stock dispersion at 5 volume % was mixed by a rotary agitator unit (Maxi-mixer) for 2 minutes, then diluted in 10^{-3} M KNO_3 solution in two stages in order to prepare low concentration (10^{-4} wt%) suspensions for particle size measurement. Ten measurements of each sample were performed and examined for particle sedimentation or drift in response with time. The particle size distribution is presented as the average of the ten measurements.

Zeta potential. A Stabino particle charge mapping instrument (ParticleMetrix, GmbH) was used to evaluate the pH titration behavior of the alumina particles and to compare the effect of PAA as a known dispersant with the lignin-derived materials. Zeta potential was measured on dilute dispersions of Sumitomo AKP-30 alumina powder (α-Al_2O_3) in 10^{-3} M KNO_3 electrolyte solution as a function of pH. The initial suspension was adjusted to pH 10 using 0.1 M KOH solution, and zeta potential vs. pH was determined using a dynamic addition profile (aliquots between 10-100 uL, and 10-25 sec between each measurement point) to titrate to pH 4 with 0.1 N HNO_3. Baseline values were determined for the as-received alumina powder and for alumina powder incubated with PAA.

Turbiscan stability index measurements. Suspensions were evaluated for stability using a Turbiscan Lab analyser. This instrument performs an optical scan over the height of the sample, measuring transmittance and backscatter via two sensors located at 180 degrees (backscatter, BS) and 45 degrees (transmittance) with respect to the pulsed IR incident beam (880 nm). For each time point transmitted and backscattered intensities are collected over the total height of the suspension. The scans are analyzed to determine the sedimentation rate of particles within the standing fluid. The temperature during the measurement was maintained at 30 °C, and the duration of the test was 12 hours. Suspensions were tested at 5 volume % alumina.

Sedimentation within the initially opaque suspension was evaluated using the backscatter profile. The difference in the measured values at each time point compared to the values from the initial scan are plotted as ΔBS versus height profiles. The behaviour of different systems are quantitatively compared using the Turbiscan Stability Index (TSI). The TSI is a measure of the dispersion stability, where a lower TSI indicates a more stable dispersion. The TSI is calculated by proprietary software using the time-dependent changes in both transmittance and backscatter over the entire height of the column.

3. Results and discussion

Solubilization of lignin from thin films by the Fenton and chelator-mediated Fenton reactions. In the initial phase of our work a large number of reactions were conducted simultaneously using an assay involving OS lignin cast as a thin film on a silicon wafer (Fig. S1),(31) allowing extensive exploration of reactant concentrations. These measurements rapidly identified conditions for the most effective use of H_2O_2

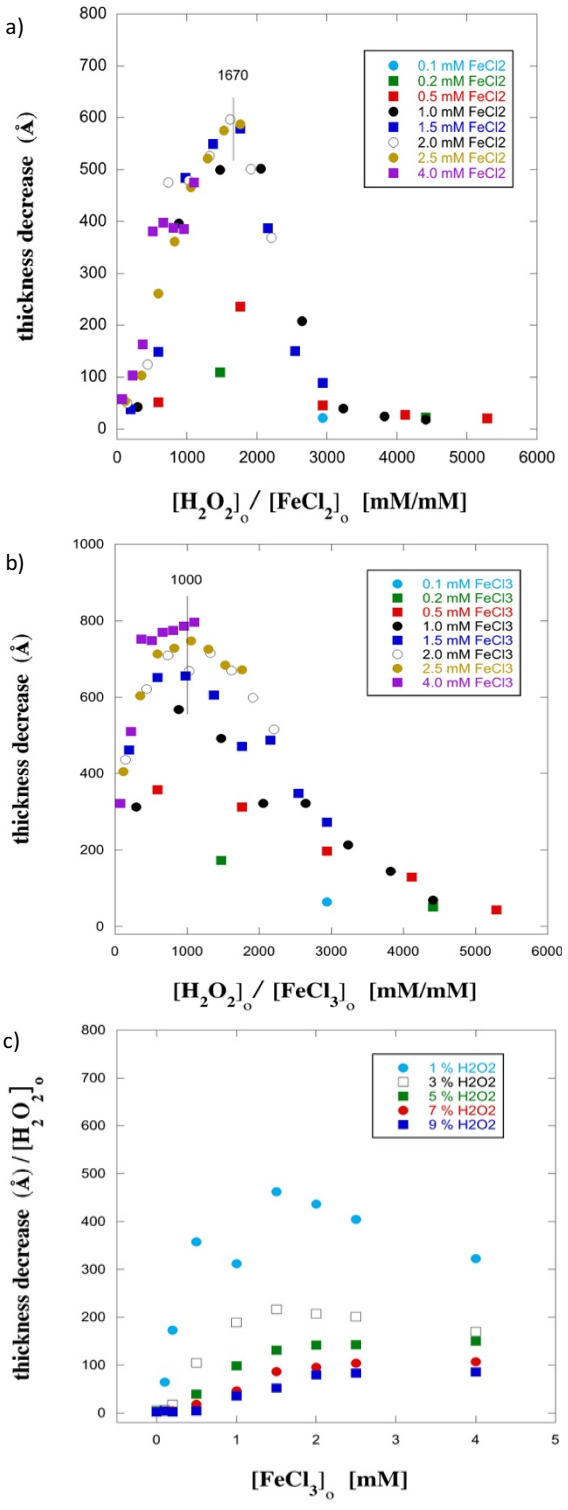

Fig. 1. a). Decrease in film thickness as a function of $[H_2O_2]_o$ / $[FeCl_2]_o$ for FEN with $[FeCl_2]_o$ ranging from 0 mM to 2.5 mM and $[H_2O_2]_o$ ranging from 1 wt % to 15 wt%. b). Decrease in film thickness as a function of $[H_2O_2]_o$ / $[FeCl_3]_o$ for CMF with $[FeCl_3]_o$ ranging from 0 mM to 4 mM and $[H_2O_2]_o$ ranging from 1 wt % to 15 wt%. c). Decrease in film thickness normalized to the concentration of H_2O_2 used for CMF as a function of $[FeCl_3]_o$.

and provided insight into the importance of non-productive reactions of hydroxyl radical with each reactant. The amount of lignin mass converted to water-soluble fragments was determined by measuring the decrease in lignin film thickness after incubation for 18 hr. Fig. 1a shows results for FEN over a wide range of both $[FeCl_2]_o$ and $[H_2O_2]_o$ (see also Fig. S2). Little lignin was solubilized from the film for $[FeCl_2]_o \leq 0.5$ mM. Mass solubilization from the film passes through a maximum as a function of each reactant concentration. The maximum occurs at a nearly constant molar ratio $[H_2O_2]_o$ / $[FeCl_2]_o$ of 1640, corresponding to a very large molar excess of H_2O_2. Prior work has shown that both H_2O_2 and Fe can react with hydroxyl radical, resulting in a maximum in reaction efficacy as a function of each reactant concentration.(27) Analogous data for CMF are shown in Fig. 1b, where 1,2-dihydroxybenzene (DHB) was used as the Fe chelator and reducer at equimolar ratio to Fe. For CMF the maximum amount of mass solubilized from the film is greater than for FEN, and occurs at a nearly constant molar ratio $[H_2O_2]_o$ / $[FeCl_2]_o$ of 1000, demonstrating that use of H_2O_2 is considerably more efficient for CMF than for FEN. This result is in agreement with prior work.(19, 32-35)

Whereas the results in Fig. 1b show that the total mass of lignin solubilized during the reaction is greatest for $[H_2O_2]_o$ / $[FeCl_2]_o$ = 1000, a more important measure of the efficiency of H_2O_2 usage is the mass of lignin solubilized per mass of H_2O_2 consumed. The data from Figure 1b are replotted in this manner in Fig 1c. Considering the high cost of H_2O_2, an economically-viable CMF process will likely have to employ this reactant in a manner that yields a high amount of product per H_2O_2 consumed, at the expense of the overall yield per reaction. Fig. 1c shows that by this measure, the efficiency of H_2O_2 use increases as $[H_2O_2]_o$ decreases, down to at least $[H_2O_2]_o$ = 1%.

Solubilization of lignin powder by CMF. Since the abovementioned work with lignin films, in agreement with prior work,(19, 32-34) showed that H_2O_2 is used more efficiently in CMF than FEN, further optimization was performed for CMF reactions with lignin powder starting from conditions derived from the film results. After each reaction, the dispersions were centrifuged, the supernatant collected, and the solid material rigorously dried and weighed to determine the amount of lignin solubilized by the reaction. In each case data were also collected for a control (no H_2O_2) and subtracted from the result for the corresponding reacting sample to give the mass of lignin solubilized by the reaction. Fig. 2 shows plots of lignin mass solubilized by CMF reactions as a function of OS lignin loading, pH, $[FeCl_3]_o$ = $[DHB]_o$, and $[H_2O_2]_o$. $[FeCl_3]_o$ and $[DHB]_o$ were maintained at an equimolar ratio following prior work.(32) Further details for these reactions are provided in the experimental section. Fig. 2a shows that the mass of lignin solubilized by the reaction (in which 40 mg of H_2O_2 were consumed) increases with lignin loading, and passes through a maximum as a function of pH. The increase in yield of soluble product with lignin loading for fixed $[H_2O_2]_o$ can be understood as an increased probability of productive reactions of hydroxyl radicals with increased lignin loading. The more complex behaviour with initial pH (see also Fig. S3) is related to the reduction of Fe(III) to Fe(II) by DHB which is affected by the pH dependent formation of Fe complexes with OH and DHB. The reduction of Fe(III) to Fe(II) by DHB and similar compounds in aqueous solution has been studied previously.(14, 19, 32-36) Prior work has shown that Fe(III) is only reduced to Fe(II) in the

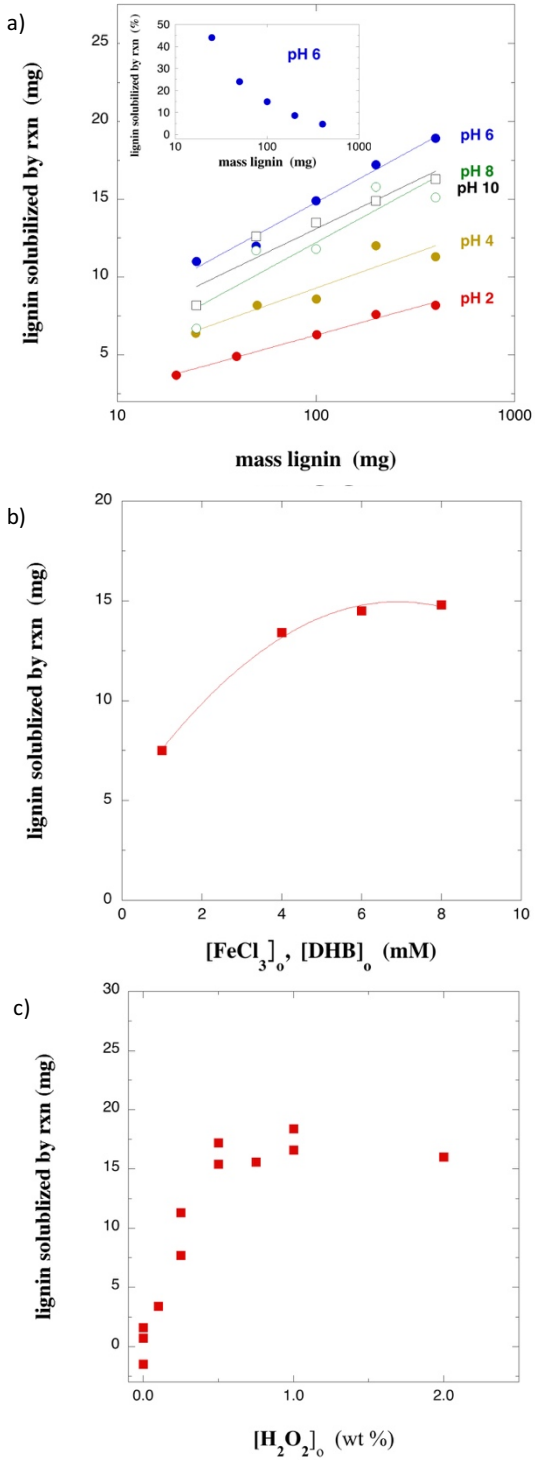

Fig. 2. Optimization of CMF reaction conditions to maximize solubilization of lignin mass as a function of a) initial pH and lignin loading at $[FeCl_3]_o$ = $[DHB]_o$ = 4 mM and $[H_2O_2]_o$ = 0.5%, b) $[FeCl_3]_o$ and $[DHB]_o$ in equimolar ratio at pH 6 and initial lignin mass of 200 mg, and c) $[H_2O_2]_o$ at pH 6, 4 mM $[FeCl_3]_o$ = $[DHB]_o$ = 4 mM, and initial lignin mass of 200 mg. The inset in a) shows the data for pH 6 expressed as percent of lignin solubilized.

monocatecholate complex, which is obtained at pH less than 5.5, whereas at higher pH formation of dicatecholate and triscatecholate complexes occurs.(35-37) However at pH below 3 formation of $Fe(OH)^{2+}$ is favoured and little $Fe(DHB)^{+}$ is formed. So an intermediate pH is required and based on the distribution of complexes in solution an optimal pH of 3.4 was predicted for degradation of the soluble monoaromatic compound veratyl alcohol in dilute solution.(32) During our reactions the pH was not held constant but rather decreased substantially. For example, for the reactions at an initial pH of 6 in Figure 2a the final pH was slightly below 3. The data in Fig. 2a refer to the pH prior to initiation of the reaction by addition of H_2O_2. The maximum in yield of solubilized lignin near initial pH of 6 shown in Fig. 2a likely occurs because this initial pH results in the greatest amount of $Fe(DHB)^{+}$ formed during the reaction. Another factor that may play a role, especially relevant to polymeric lignin, is that oxidized lignin fragments are more soluble at higher pH. The inset to Figure 2a shows the data for initial pH of 6 expressed as percent of lignin solubilized. A tradeoff exists between the percent of lignin solubilized and the efficiency of H_2O_2 use (mass of lignin solubilized per mass of H_2O_2 consumed).

Fig. 2b and Fig. 2c show the variation in solubilized lignin mass with $[FeCl_3]_o$ = $[DHB]_o$ and $[H_2O_2]_o$, respectively. With respect to both reactant concentrations, the yield of solubilized lignin increases strongly followed by a plateau where further increase in $[FeCl_3]_o$ = $[DHB]_o$ or $[H_2O_2]_o$ has no impact on the yield of lignin solubilized. This contrasts with the results of the lignin film assay where the amount of mass solubilized by the reaction goes through a distinct maximum with increasing concentration of each reagent. Another important difference between the powder and film assay results is that in both Fig. 2b and Fig. 2c the onset of the plateaus occur at a molar ratio $[H_2O_2]_o$ / $[FeCl_3]_o$ of ~36, a much lower value than the reactant ratio at the maximum in the film assay (1000, Fig 1b). These differences are likely due to the very large difference in lignin accessible surface area in the two cases along with the difference in the distribution of lignin mass within the reaction volume. The mass of lignin per reaction volume was more than 1000 times greater in the lignin powder-dispersion reactions than in the reactions with lignin films. This, combined with the fact that the lignin was dispersed throughout the reaction volume in the powder reactions but was not dispersed in the film assay, resulted in a much greater accessible lignin surface area in the lignin powder reactions. The latter affects the relative probabilities of non-productive and productive reactions of hydroxyl radicals. We believe that the film reactions represent a limiting case with high probability of non-productive reactions of hydroxyl radical with either H_2O_2 or Fe. Since the solutions in the wells were not stirred during the incubation period and the device was left at rest (not on a shaker), the majority of reactants had to diffuse a macroscopic distance (several mm) to encounter the lignin substrate. At sufficiently high concentrations of either H_2O_2 or Fe, non-productive reactions of hydroxyl radical with that reactant begin to dominate leading to well-defined maxima in the reaction yield with either reactant concentration. In the reactions with dispersed lignin powder the probability of an hydroxyl radical participating in a productive reaction with lignin, as opposed to non-productive reactions with H_2O_2, Fe, or other species, is much greater compared with reactions in the film assay. This is shown by the fact that H_2O_2 is used much more efficiently in the case of the dispersions of lignin powder (molar ratio $[H_2O_2]_o$ / $[FeCl_3]_o$ of 36 compared with 1000 in the film assay). For comparison, an optimal ratio of 95-290 was reported by Gulkaya et al. for FEN treatment of wastewater.(27) We suggest that these various optimal ratios of $[H_2O_2]_o$ / $[FeCl_3]_o$ reflect differences in reaction conditions that result in differing probabilities for non-productive reactions of hydroxyl radical.

Other Fe chelators/reducers were also examined. Results for 2,3-dihydroxybenzoic acid, and 1,2,3 trihydroxybenzene are given in Supporting Information Fig. S4. DHB gave the highest yield of the three Fe chelators/reducers at pH 6. It is interesting to note that DHB gave higher yield than DHBA despite the fact that the kinetics of Fe(III) reduction are faster for DHBA than for DHB (reactions performed at pH 4.5).(14) Our data suggests that the higher yield of water-soluble material with DHB is due to a stronger association of DHB with lignin than for the more soluble DHBA. Stronger association of the Fe(DHB) complex with lignin was indicated in the control measurements performed in absence of added H_2O_2. In these measurements, the mass of the Fe(DHB) complex was detected with the insoluble lignin (yielding a total insoluble mass that was greater than that of the initial mass of lignin). On the other hand, for DHBA the mass of the Fe(DHBA) complex was not detected with the insoluble lignin, indicating that the complex remained soluble. For a chelator/Fe(III) complex that is sparingly soluble and associates with lignin, it is more likely that hydroxyl radical will be generated in the immediate vicinity of lignin and participate in a productive reaction with lignin. This may explain the higher yield for DHB than for DHBA.

Prior work has shown that upon interaction of hydroxyl radical with an aromatic ring to form a cyclohexadienyl radical, ring opening is favoured over other decay pathways in the presence of dissolved O_2.(11) Therefore, we postulated than the yield of solubilized lignin may increase with air or O_2 bubbling during the reaction. To test this hypothesis a series of reactions were performed with and without bubbling of 100% O_2 (0.05 standard cubic feet per hour) with 100 mg lignin in 8 mls, $[H_2O_2]_o$ = 0.5%, and $[FeCl_3]_o$ = $[DHB]_o$ = 4 mM at initial pH 6. The reactions and controls (no H_2O_2) were performed in triplicate. The results, shown in Supporting Information Fig. S5, indicate a 45% increase in yield of solublized lignin with O_2 bubbling relative to that in absence of O_2 bubbling.

Further improvements in yield and in the economics of this process are likely to be possible. The lignin loading can be increased by at least a factor of 2 over the highest value shown in Figure 2 (400 mg / 8 ml = 5%). At much higher lignin loadings, a high viscosity may render the process intractable. The data in Figure 2a indicate that a higher lignin loading will result in a higher yield of solubilized lignin per H_2O_2 consumed. In addition, it is likely that DHB could be added at less than equimolar ratio to $FeCl_3$ since de-methoxylation and conversion to a phenolic hydroxyl can occur for lignin subunits in the presence of

hydroxyl radical (13, 38-40) and will generate dihydroxy aromatic moieties. Prior data has suggested that some dihydroxy aromatic Fe chelators are able to reduce Fe^{3+} to Fe^{2+} up to 5-6 times.(21) Given the large molar excess of aromatic rings of lignin compared with the Fe in our reactions, lignin has great capacity to reduce Fe(III) to Fe(II) and therefore it is likely that DHB could be added in less than equimolar amounts with respect to $FeCl_3$. Finally, the yields of solubilized lignin per mass of H_2O_2 consumed reported in Fig. 2 are for single batch reactions. Higher values were obtained when successive reactions were performed (see Methods section for details). In particular, up to 0.6 g of lignin solubilized per g of H_2O_2 consumed and up to 10% of lignin solubilized per reaction were obtained at 5% lignin loading, and up to 0.8 g lignin solubilized per g of H_2O_2 consumed and up to 4% of lignin solubilized per reaction were obtained at 10% lignin loading. These results were obtained in absence of O_2 bubbling.

CMF reactions were also performed with Kraft, IL, and DMR-EH lignins. The yields obtained for these lignins were comparable to that for OS lignin (Fig S6).

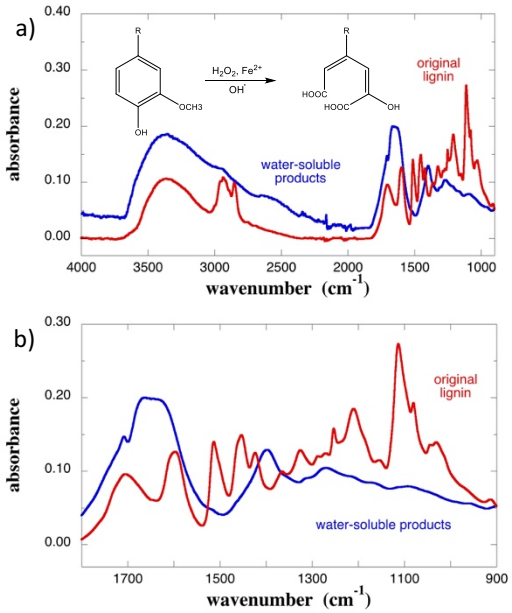

Fig. 3. a). FTIR spectrum from OS lignin solubilized by CMF reaction at $[FeCl_2]_o$ = 4 mM and $[H_2O_2]_o$ = 0.5% compared with spectrum from original lignin. The reaction was performed with initial pH of 10 and 100 mg lignin in 8 ml total volume. The inset shows the proposed reaction scheme. b). Expansion of the fingerprint region.

Chemical analysis of solubilized products. Chemical changes in the lignin that occurred upon CMF reaction were determined by FTIR spectroscopy. Results for a representative reaction condition are shown in Fig. 3. Absorbance bands were assigned following prior work.(41-43) For the material rendered water-soluble by the reaction, bands associated with the aromatic rings (aromatic skeletal vibrations at 1598 cm^{-1}, 1514 cm^{-1}, and 1425 cm^{-1}, aromatic C-H stretch at 1114 cm^{-1} in S units (41, 42, 44, 45)) are nearly entirely absent. In addition, strong bands for the original lignin at 2800-3000 cm^{-1}, 1460 cm^{-1}, and 1211 cm^{-1} are also absent for the water-soluble post-reaction material. The bands at 2800-3000 cm^{-1} and 1460 cm^{-1} correspond, respectively, to C-H stretch and C-H deformation of methyl and methylene groups.(41, 46, 47) We assign the band at 1211 cm^{-1} to aryl-O stretching mode of the aromatic ether.(46) The absence of these bands in the water-soluble product indicates loss of the methoxy groups. Oxidation of the methoxy groups of lignin to form aryl hydroxyl units with methanol as a by-product has been reported previously.(13) For the water-soluble post-reaction material new bands are present at 1674 cm^{-1}, 1614 cm^{-1}, and 1406 cm^{-1}. The bands at 1674 cm^{-1} and 1614 cm^{-1} are indicative of carbonyl and carboxyl groups conjugated with alkenes.(41, 48) We assign the new band at 1406 cm^{-1} to the symmetric carboxylate C-O vibration.(49, 50). These new bands after reaction are consistent with formation of carboxylic acids upon cleavage of the aromatic rings. Carboxylate complexes with Fe (50) may form upon drying of films for FTIR-ATR measurements. A proposed scheme for CMF reaction with aromatic moities in lignin is shown in the inset to Fig 3a.

FTIR spectra for CMF reactions for a range of lignin loading and for a range of initial pH, with $[FeCl_2]_o$ = $[DHB]_o$ = 4 mM and $[H_2O_2]_o$ = 0.5% are shown in Fig. S7 and Fig. S8. These spectra are similar to the spectra in Fig. 3, indicating that little variation in the chemical nature of the water-soluble material occurs as a function of either initial pH (from 4 – 10) or lignin loading.

FTIR spectra for KRAFT, DMR-EH, IL and OS lignins after CMF reaction with $[FeCl_2]_o$ = $[DHB]_o$ = 4 mM, $[H_2O_2]_o$ = 0.5% initial pH of 6, and 50 mg lignin per 8 mls total volume are shown in Fig. S9. The spectra are very similar for these four lignins, showing nearly complete ring-opening, loss of methoxy groups, and formation of carbonyl or carboxyl groups conjugated with alkenes in each case.

2D ^{1}H-^{13}C HSQC NMR spectra for the original OS lignin and the water-soluble post-reaction material are shown in Fig 4a. The spectra indicate complete absence of aromaticity in the water-soluble post-reaction material. The data also show a dramatic decrease in the methoxy resonance at 55 PPM / 3.8 PPM. The direct ^{13}C NMR spectra in Fig S9 confirm the loss of aromaticity (loss of resonances from 130 ppm -155 ppm) and show resonances at 175 ppm and 126 ppm consistent with the presence of COOH conjugated with alkenes for the post-reaction water-soluble material.

NaOH titration of the lignin-derived material from a reaction with $[FeCl_2]_o$ = $[DHB]_o$ = 4 mM and $[H_2O_2]_o$ = 0.5% at initial pH of 6 indicated 6 mmol/g or roughly 1 COOH per lignin monomer, assuming a monomer molecular weight of 160 g/mol. This amount of carboxylic acid groups is much higher than achieved with other oxidative processes that result in only partial ring opening.(47, 51) There is little evidence for carboxylic acids in the original OS lignin, as no peaks are present at 1670 cm^{-1} or 1400 cm^{-1} in the FTIR spectrum (Fig 3) and no resonances are present in the range of 175-185 PPM in the C13 NMR spectrum where the carboxylic acid peaks occur for polyacrylic acid and for the ring-opened lignin-derived material.

Given the above evidence that solublization occurs through opening of the aromatic rings to produce acid groups, we next present an estimate of the theoretical maximum yield of lignin per amount of H_2O_2 consumed. One molecule of H_2O_2 will produce one hydroxyl radical in the Fenton reaction.(11, 15) At high H_2O_2 concentrations hydroxyl radical can react with H_2O_2, decreasing the amount of H_2O_2 available to oxidize lignin. However, in our process the concentration of H_2O_2 is always kept sufficiently low (~0.5%) such that that reaction should be negligible. In the presence of dissolved O_2, one hydroxyl radical is sufficient to open the ring of one lignin monomer.(11) The mole ratio of 1 molecule H_2O_2 per 1 aromatic ring opened corresponds to a mass ratio of 1 g H_2O_2 per 4.7 g lignin, assigning 160 g/mol per lignin monomer. However hydroxyl radicals attack lignin subunits by abstracting aliphatic C_α hydrogens as well as by adding to aromatic rings.(38) Based on the molecular weight ratio of an aromatic ring to the total mass of a lignin monomer we estimate that only half the radicals that interact with lignin will add to an aromatic ring. If an hydroxyl radical adds to an aromatic ring at the site of a methoxy group the most likely effect is release of methanol rather than ring opening.(38) Likewise, if a hydroxyl radical adds to an aromatic ring at the site of a β-O-4 ether linkage the most likely effect is cleavage of the ether bond. Assuming on average one methoxy group and one β-O-4 ether linkage per aromatic ring, only four sixths of the reactions of hydroxyl radical with aromatic rings will result in ring opening. Therefore, we estimate a theoretical mass yield of 4.7 g lignin x (1/2) x (4/6) or 1.6 g lignin solubilized per 1 g H_2O_2 consumed. This assumes nearly all the rings must be opened to solubilize lignin, which is consistent with our FTIR data showing complete absence of the aromatic bands for the material solubilized at these low pH conditions. The fact that the pH was low (<3) after reaction is consistent with the observation that most of the rings were opened in the water-soluble material. If the pH were maintained at a higher value during the reaction, we expect that lignin polymers with only a fraction of the rings opened would be soluble. The estimated theoretical mass ratio of 1.6 g polyacid product per 1 g H_2O_2 consumed is 3.2 times greater than the best mass ratio shown in Fig 2 of 0.5 g polyacid product per 1 g H_2O_2 for individual batch reactions. However, considering a mass ratio of polyacid product per H_2O_2 consumed of 0.8 achieved for multiple successive reactions and a further 45% increase in yield with O_2 bubbling, we conclude that mass ratios greater than 1 are achievable.

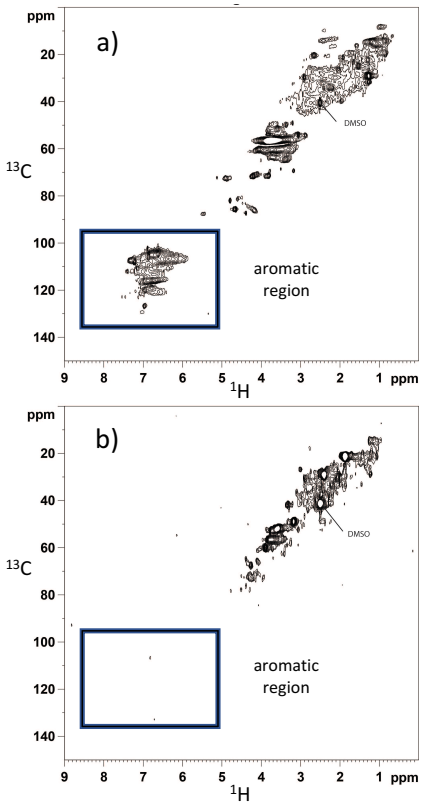

Fig. 4. ^{1}H-^{13}C 2D HSQC NMR spectra for a) the original OS lignin and b) the water-soluble post-reaction material for CMF reaction with $[FeCl_2]_o$ = 4 mM and $[H_2O_2]_o$ = 0.5%, initial pH of 6, and 100 mg lignin in 8 ml total volume.

Molecular weight distribution of solubilized products. For certain applications, such as plasticizing concrete (52, 53) or dispersing inorganic particles in aqueous suspensions (54, 55), the molecular weight distribution of the polyacid material is very important. The molecular weight distribution of the water-soluble material derived from CMF reactions was characterized by aqueous phase GPC with UV detection at 210 nm. A detection wavelength of 210 nm was chosen since the IR data indicates that the aromatic rings, with UV peak near 260-280 nm, are opened during the reaction.

Fig. 5a shows the MW distribution for water-soluble material from a CMF reaction with $[FeCl_2]_o$ = $[DHB]_o$ = 4 mM and $[H_2O_2]_o$ = 0.5% at an initial pH of 6 and lignin loading of 12.5 mg/ml. The molecular weight distribution is compared with that of the original material determined by GPC using THF as the mobile phase. The results indicate that some lower molecular weight species are generated by the reaction. However, the majority of the water-soluble material has molecular weight comparable to that of the original lignin. The molecular weight distributions for a range of lignin loading and initial pH, with $[FeCl_2]_o$ = $[DHB]_o$ = 4 mM and $[H_2O_2]_o$ = 0.5%, are shown in Fig. 5b and Fig. 5c. Only relatively small variations in the molecular weight distribution of the water-soluble material occur as a function of either pH or lignin loading. In particular, the lower molecular weight portion of the distribution decreases in magnitude with increase in lignin loading whereas some polymerization occurs at the lowest lignin loading indicated by the presence of a high molecular weight shoulder. Finally, we note that very little change in the molecular weight distribution of the water-souble product occurred with successive reactions.

These results show that the molecular weight distribution of the water-soluble product is similar to that of the original material. Therefore, for specific applications the desired molecular weight distribution can be achieved by selecting appropriate initial lignin fractions for the CMF reaction.

Dispersant characteristics of lignin solubilized by CMF reaction. While there are many potential applications for this water-soluble polyacid derived from lignin, here we demonstrate the performance of the material as a dispersant. Fig. 6 presents zeta potential measurements for alumina after incubation with the lignin product from CMF with $[FeCl_2]_o$ = $[DHB]_o$ = 4 mM and $[H_2O_2]_o$ = 0.5% and initial pH of 6 compared with results for the alumina after incubation with poly(acrylic acid) with Mw = 2000 g/mol. For both PAA and the lignin-derived dispersant, increasing concentration of the dispersant leads to a shift in the isoelectric point (IEP) to lower pH values. For both dispersants the IEP decreases to pH 4 for 4 mg dispersant/g alumina. For the lignin-derived dispersant, the zeta potential measured at pH 9 (-50 mV) was greater in magnitude than that provided by PAA. From an electrosteric stabilization standpoint, the performance and behaviour of the lignin-derived polyacid and PAA are comparable. These zeta potential results suggest that the polyacid product from CMF reactions perform as well or better than poly(acrylic acid) (PAA) with respect to dispersing alumina particles.

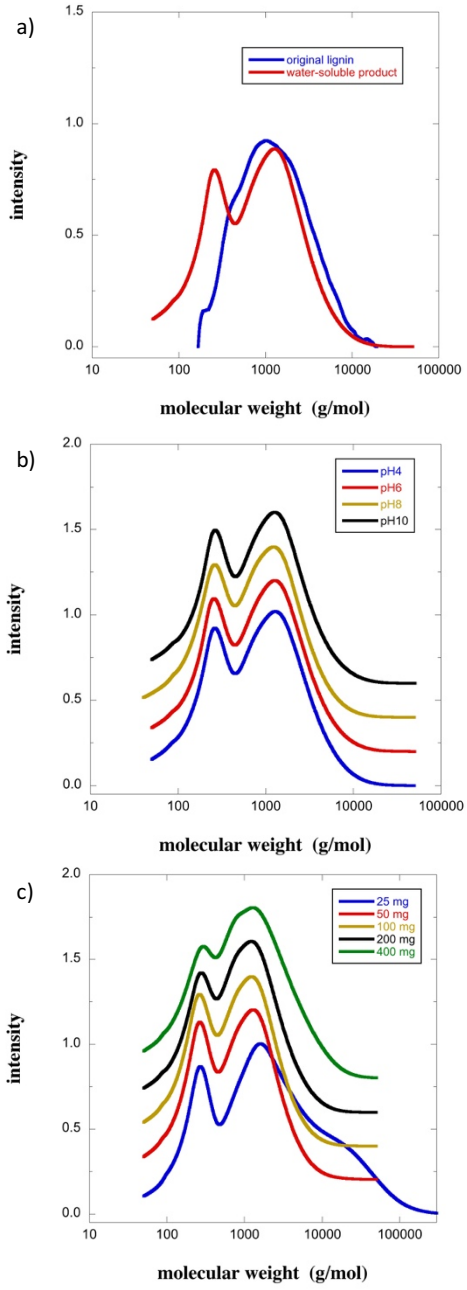

Fig. 5. a) Molecular weight distribution of lignin solubilized by CMF reaction at $[FeCl_2]_o$ = 4 mM and $[H_2O_2]_o$ = 0.5% compared with the molecular weight distribution of the unreacted lignin. The reactions were performed with initial pH of 6 and a lignin loading of 12.5 mg/ml. b) Molecular weight distribution for the same reactions conditions but with various initial pH values. b) Molecular weight distribution for the same reactions conditions but with different lignin mass loadings (per 8 ml total).

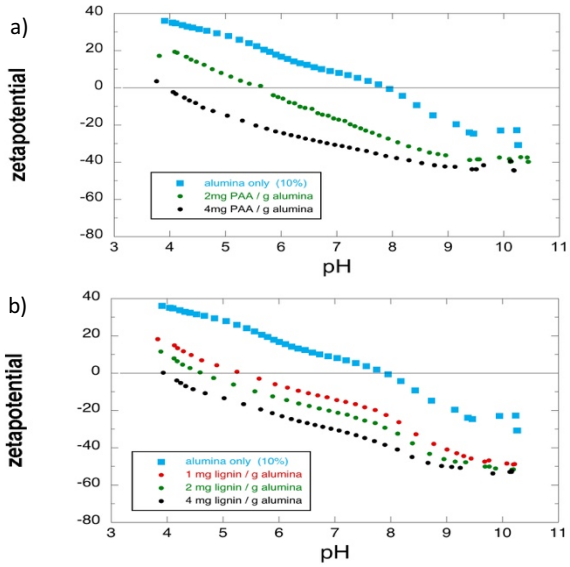

Fig. 6. a). Zeta potential versus pH for AKP-30 alumina alone and after incubation with increasing concentrations of a) PAA and b) Lignin-derived material from CMF with 4 mM ($FeCl_3$+DHB) and 0.5% H_2O_2.

Fig. 7a shows alumina particle size distribution (PSD) measurements taken for samples of the two dispersants at pH 9 to represent the electrosterically repulsive interaction, and at the IEP for the dispersant to examine the flocculated state. The PSD measurements indicate comparable dispersion behaviour for the two systems. At pH 9 where both dispersants generate sizeable repulsive electrosteric interactions, the particles are dispersed with a skewed distribution having a mean size near 600 nm. Likewise, at the IEP of the system, the particles are flocculated with a mean size near 1600 nm, indicating that attractive interactions lead to weak association of the particles. This flocculated size is similar to that of the as-received alumina at the IEP (Fig. 7b). The data in Fig. 7a shows that the two additives have comparable dispersing power.

The contrast between electrosterically-stabilized systems and systems flocculated at the IEP was further examined using turbidimetry scanning. Fig. 8 shows successive backscattered scans of each system over 12 h. Both the PAA and lignin-derived dispersants exhibit sedimentation behavior at the IEP, and

slower, gravity-induced fractionation for the electrosterically-stabilized condition. Fig. 8a and Fig. 8c contrast the sedimentation rate behavior between PAA and lignin-derived polyacid at the IEP, where electrostatic stabilization is absent and the steric layer of the particles alone acts against van der

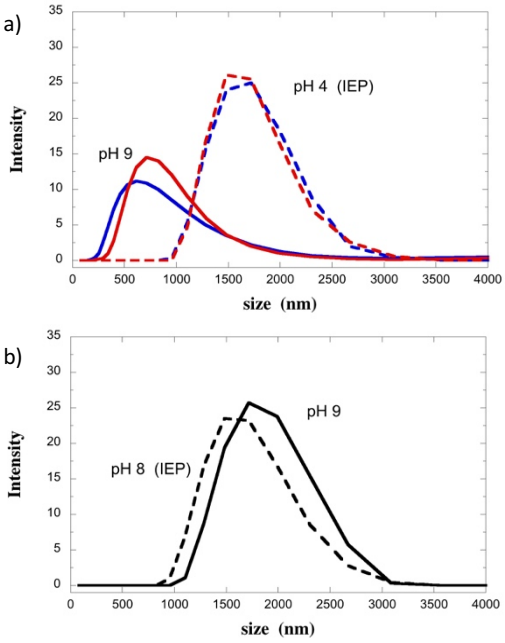

Fig. 7. a). Particle size distribution at pH 9 (solid lines) and pH 4 (IEP) (dashed lines) for AKP-30 alumina treated with 4 mg PAA/g alumina (blue) or with 4 mg lignin-derived material/g alumina (red). b). Corresponding data for untreated AKP-30.

Waals attraction between alumina particles. The PAA sample sedimented uniformly across the sample to approximately half the initial height of the sample over the course of 3 h, after which little further sedimentation occurred. This corresponds to densification to a particle concentration of approximately 10% from the initial slurry value of 5%. This suggests that the floc structure is relatively open, based on the normative value of 16% for the development of a percolation structure in a particle gel.(56) In contrast, the lignin polyacid undergoes more rapid sedimentation to a more concentrated particle structure having one third the initial volume, and giving a particle concentration of approximately 15%. This is more consistent with percolation theory for the spanning volume fraction in a hard sphere particle system. We suggest that there is a weak attractive force between the PAA samples that is absent in the lignin polyacid, based on steric dispersion of the adsorbed polymer layer. Potentially, the more random or branched molecular structure of the lignin polyacid creates a thicker steric layer than flat adsorption of a linear PAA chain. The van der Waals attractive forces would be mitigated between surfaces with thicker steric layers, and thus induce better stabilizing forces between the powders.

In the case of each suspension stabilized at pH 9, little sedimentation was observed in the optical profile of the suspension, with a small portion of the sample at the top becoming gradually more transmissive. This is induced by gravimetric sedimentation of the particle distribution, and indicates that the finest particle are stabilized by thermal forces over the period of time examined. This behaviour is consistent with the zeta potential values for each system, in which strong electrosteric stabilization is indicated for both dispersants. To quantitatively compare the dispersion stability of each system, Fig. 9 displays the Turbiscan Stability Index (TSI) for each condition. From Fig. 9a, the behaviour of each system at pH 9 is nearly identical and indicates strong particle-particle repulsion. The stability index is linear, indicating that gravity-induced

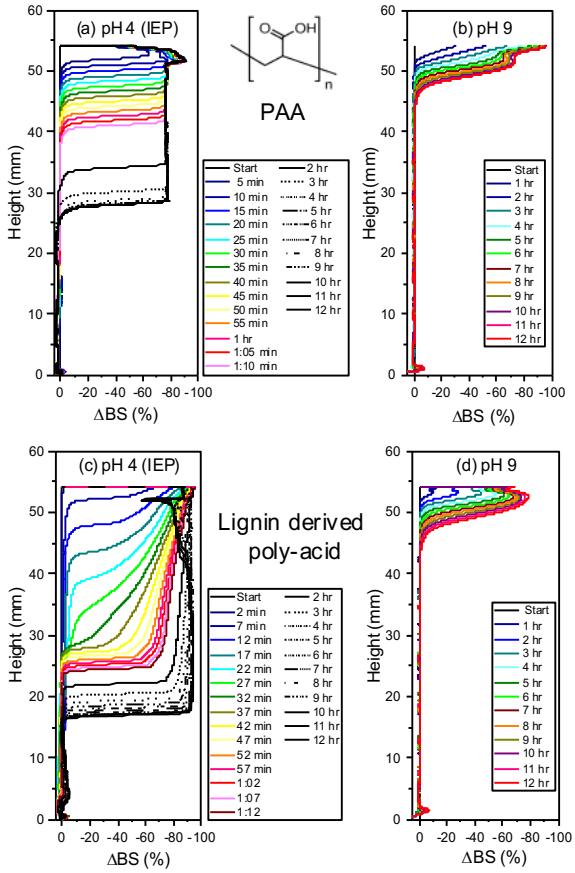

Fig. 8. Turbiscan ΔBS profiles for 5 vol % alumina suspensions vs. time at 30 C for alumina treated with either PAA (a, b) or lignin-derived material from CMF (4 mM ($FeCl_3$+DHB) + 0.5% H_2O_2) c, d). Measurements were performed at pH 4 (IEP) (a, c) and at pH 9 (b, d).

settling is the only phenomena observed here. In contrast, at pH 4 (the IEP) the two systems differ. PAA destabilized rapidly, and after 4 hours did not further consolidate. This indicates the formation of a gel structure. The lignin-derived polyacid shows rapid destabilization within the first hour, but continues to consolidate over time. The continued densification over time shows that the attraction between these samples is weaker, and the particle bed can restructure over time to achieve greater densification. This is consistent with the interpretation that the lignin has a thicker adsorbed layer which reduces particle-particle adhesion, allowing for greater densification upon sedimentation.

Comparison with lignosulfonates. Lignosulfonates (LS) are water-soluble polymers derived from lignin, and can be compared with the lignin-derived polyacid material reported in this work. LS are produced from sulphite pulping and from sulphite pre-treatment of lignocellulosic biomass in biorefineries.(57, 58) By far the largest use of LS has been as plasticizers/dispersants of cement in concrete,(53, 58, 59) but LS has also been explored for use as a binder in manufacture of fibreboard,(58, 60) as a viscosity reducer in oil drilling, and as a dispersant of inorganic particles such as dyes, pesticides, ceramics, and graphite,(57) among others.(58) Sulphite pre-treatment of lignocellulosics produces biorefinery LS. Some of the abovementioned applications require high molecular weight, and the FEN reaction has been explored for increasing the molecular weight of lignosulfonates.(53) Compared to the sulfite process, our approach provides an alternative route to convert lignin into a water-soluble polyacid that is compatible with a wide range of biomass pretreatment approaches and is more environmentally friendly, as sulphite processes release SOx. Altering reaction conditions or adding further processing or chemical steps to increase the molecular weight of the polyacid product is likely to be possible, but is outside the scope of the present work.

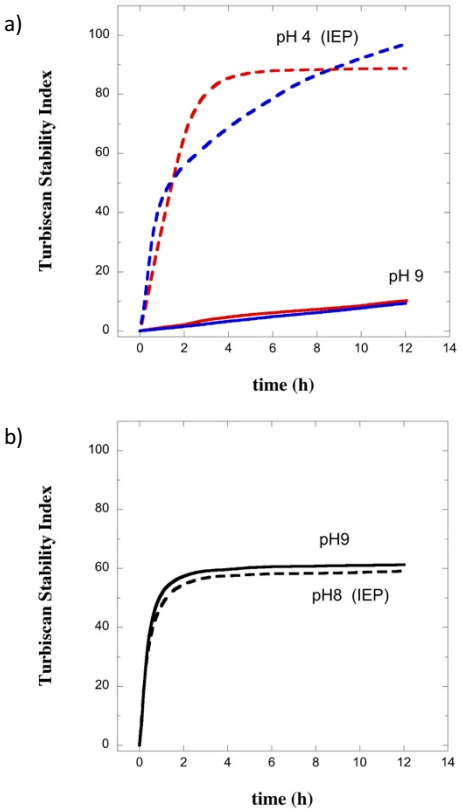

Fig. 9. a). Turbiscan stability index values at pH 9 (solid lines) and pH 4 (IEP) (dashed lines) for AKP-30 alumina treated with 4 mg PAA/g alumina (blue) or with 4 mg lignin-derived material/g alumina (red). b). Corresponding data for untreated AKP-30.

Conclusions

We report an efficient CMF process that chemically opens the aromatic rings of lignin to form acid groups, resulting in a water-soluble polyacid. The present work contrasts with prior work involving FEN and CMF by using only sparing amounts of H_2O_2 in the presence of a large excess of lignin to minimize unproductive reactions of hydroxyl radical and maximize the amount of product formed per H_2O_2 consumed. This could be achieved in a semicontinuous reactor. The present work also contrasts with other H_2O_2-based oxidative treatments (47, 51) in achieving nearly complete ring opening. Our results indicate a yield of greater than 1 g polyacid per g H_2O_2 consumed is achievable. We note that it is possible to generate H_2O_2 in-situ enzymatically by converting either methanol (generated from oxidation of methoxy groups)(61) or residual sugars (62, 63) into H_2O_2. Comparable yields and extent of ring–opening were observed for KRAFT, IL, DMR-EH, and OS lignins, showing that the results are broadly applicable to many types of lignin. We demonstrated the usefulness of the OS lignin-derived polyacid material as a dispersant for alumina particles, showing that the performance is comparable to a commercial polyacrylic acid of similar weight averaged molecular weight. Considering that the bulk selling price of PAA ($2200/metric ton) is more than twice that of H_2O_2 ($400/metric ton for 50% solution), this approach holds promise for generating value from lignin.

Conflicts of interest

There are no conflicts to declare.

Author Contribution

M. S. K. conceived and designed the experiments, and supervised the overall project. J. Z. performed aqueous GPC measurements, provided insights into Fenton chemistry, and contributed to analysis of results and interpretation. N. C. R. performed solubilization assays with lignin films and lignin powders and performed light scattering measurements. I. A. performed solubilization assays with lignin films. C. T. S. performed solubilization assays with lignin films and lignin powders. C. K. B. performed molecular weight analysis by aqueous GPC. M. L. B. developed an automated system for ellipsometric measurements of film thicknesses in the lignin film assay and supervised those measurements, J. D. W performed molecular weight analysis of the original lignin using GPC with THF as running solvent. N. H. G. performed the FTIR measurements. T. M. A. performed the NMR measurements. M. D. A. and B. A. S. consulted on the overall project. N. S. B. performed Turbiscan and zetapotential measurements and consulted on data analysis and interpretation. K. L. S. consulted on the overall project and contributed to analysis of results and interpretation. The manuscript was mainly written and revised by M. S. K. and K. S. L. All authors contributed to the discussion of the results and commented on the manuscript.

Acknowledgements

This work was part of the DOE Joint BioEnergy Institute (http://www.jbei.org) supported by the U.S. Department of Energy, Office of Science, Office of Biological and Environmental Research, through contract DE-AC02-05CH11231 between Lawrence Berkeley National Laboratory and the U.S. Department of Energy. This work was also supported by the Laboratory Directed Research and Development program at Sandia National Laboratories. Sandia National Laboratories is a multi-mission laboratory managed and operated by National Technology and Engineering Solutions of Sandia, LLC., a wholly owned subsidiary of Honeywell International, Inc., for the U.S. Department of Energy's National Nuclear Security Administration under contract DE-NA-0003525. Part of this work was performed at the Center for Integrated Nanotechnologies, a US Department of Energy, Office of Basic Energy Sciences user facility at Low Alamos National Laboratory (contract DE-AC52-06NA25396) and Sandia National Laboratories. We thank Mat Celina for assistance with the FTIR measurements.

Notes and references

1. **Simmons BA, Loque D, Ralph J.** 2010. Advances in modifying lignin for enhanced biofuel production. Curr Opin Plant Biol **13:**313-320.
2. **Zakzeski J, Bruijnincx PCA, Jongerius AL, Weckhuysen BM.** 2010. The catalytic valorization of lignin for the production of renewable chemicals. Chemical Reviews **110:**3552-3599.
3. **Pandey MP, Kim CS.** 2011. Lignin depolymerization and conversion: A review of thermochemcial methods. International Journal of Biochemistry and Molecular Biology **34:**29-41.
4. **Ragauskas AJ, Beckham GT, Biddy MJ, Chandra MJ, Chen F, Davis MF, Davison BH, Dixon RA, Paul G, Keller M, Langan P, Naskar AK, Saddler JN, Tschaplinski TJ, Tuskan GA, Wyman CE.** 2014. Lignin valorization: improving lignin processing in the biorefinery. Science **344:**1246843.
5. **Linger JG, Vardon DR, Guarnieri MT, Karp EM, Hunsinger GB, Franden MA, Johnson CW, Chupka G, Strathmann TJ, Pienkos PT, Beckham GT.** 2014. Lignin valorization through integrated biological funneling and chemical catalysis. Proc Nat Acad Sci **111:**12013-12018.
6. **Beckham GT, Johnson CW, Karp EM, Salvachúa D, Vardon DR.** 2016. Opportunties and challenges in biological lignin valorization. Current Opinion in Biotechnology **42:**40-53.
7. **Abdelaziz OY, Brink DP, Prothmann J, Ravi K, Sun M, García-Hidalgo J, Sandahl M, Hulteberg CP, Turner C, Lidén G, Gorwa-Grauslund MF.** 2016. Biological valorization of low molecular weight lignin. Biotechnology Advances **34:**1318-1346.
8. **Rodriguez A, Salvachúa D, Katahira R, Black BA, Cleveland NS, Reed M, Smith H, Baidoo EEK, Keasling JD, SImmons BA, Beckham GT, Gladden JM.** 2017. Base-catalyzed depolymerization of solid lignin-rich streams enables microbial conversion. ACS Sustainable Chemistry & Engineering **5:**8171-8180.
9. **Li Q, Xie S, Serem WK, Naik MT, Liu L, Yuan JS.** 2017. Quality carbon fibers from fractionated lignin. Green Chemistry **19:**1628-1634.
10. **Goodell BQ, Y.; Jellison, J.; Richard, M.; Qi, W.** 2002. Lignocellulose oxidation by low molecular weight metal-binding compounds isolated from wood degrading fungi: A comparison of brown rot and white rot systems and the potential application of chelator-mediated Fenton reactions, p 37-46. *In* Viikari LL, R. (ed), Biotechnology in the Pulp and Paper Industry, vol 21. Elsevier Science.
11. **Chen R, Pignatello J.** 1997. Role of quinone intermediates as electron shuttles in Fenton and photoassisted Fenton oxidations of aromatic compounds. Environ Sci Technol **31:**2399-2406.
12. **Walling C.** 1975. Fenton's reagent revisited. Accounts of Chemical Research **8:**125-131.
13. **Arantes V, Milagres AMF, Filley TR, Goodell B.** 2011. Lignocellulosic polysaccharides and lignin degradation by wood decay fungi: the relevance of nonenzymatic Fenton-based reactions. J Ind Microbiol Biotechnol **38:**541-555.
14. **Aguiar A, Ferraz A.** 2007. Fe^{3+} and Cu^{2+} -reduction by phenol derivatives associated with Azure B degradation in Fenton-like reactions. Chemosphere **66:**947-954.
15. **Kang N, Lee DS, Yoon J.** 2002. Kinetic modeling of Fenton oxidation of phenol and monochlorophenols. Chemosphere **47:**915-924.
16. **Mijangos F, Varona F, Villota N.** 2006. Changes in solution color during phenol oxidation by Fenton reagent. Environ Sci Technol **40:**5538-5543.
17. **Bissey LL, Smith JL, Watts RJ.** 2006. Soil organic matter-hydrogen peroxide dynamics in the treatment of contaminated soils and groundwater using catalyzed H_2O_2 propagations (modified Fenton's reagent). Water Research **40:**2477-2484.
18. **Araujo E, Rodriguez-Malaver AJ, Gonzalez AM, Rojas OJ, Penaloza N, Bullon J, Lara MA, Dmitrieva N.** 2002. Fenton's reagent - mediated degradation of residual Kraft black liquor. Appl Biochem Biotechnol **97:**91-103.
19. **Rodriguez J, Contereras PC, Freer J, Baeza J.** 2001. Dihydroxybenzenes: driven Fenton reations. Water Sci Technol **44:**251-256.
20. **Sun Y, Fenster M, Yu A, Berry RM, Argyropolous DS.** 1999. The effect of metal ions on the reaction of hydrogen peroxide with Kraft lignin model compounds. Can J Chem **77:**667-675.
21. **Arantes VB, C.; Milagres, A.M.F.** 2006. Degradation and decolorization of a biodegradable-resistant polymeric dye by chelator-mediated Fenton reactions. Chemosphere **63:**1764-1772.
22. **Mae K, Hasegawa I, Sakai N, Miura K.** 2000. A new conversion method for recovering valuable chemicals from oil palm shell wastes utilizing liquid-phase oxidation with H_2O_2 under mild conditions. Energy & Fuels **14:**1212-1218.
23. **Kato DM, Elia N, Flythe M, Lynn BC.** 2014. Pretreatment of lignocellulosic biomass using Fenton chemistry. Bioresource Technology **162:**273-278.
24. **Amarante D.** 2000. Applying in-situ chemical oxidation. Pollution Engineering **32:**40-42.
25. **Covinich LG, Bengoechea DI, Fenoglio RJ, Area MC.** 2014. Advanced oxidation processes for wastewater treatment in the pulp and paper industry: A review. American Journal of Environmental Engineering **4:**56-70.

26. **Tang WZ, Huang CP.** 1997. Stochiometry of Fenton's reagent in the oxidation of chlorinated aliphatic organic pollutants. Environmental Technology **18:**13-23.
27. **Gulkaya I, Surucu GA, Dilek FB.** 2006. Importance of H_2O_2/Fe^{2+} ratio in Fenton's treatment of a carpet dyeing wastewater. Journal of Hazardous Materials **B136:**763-769.
28. **Huang Y-H, Huang Y-F, Chang P-S, Chen C-Y.** 2008. Comparative study of oxidation of dye-Reactive Black B by different advanced oxidation processes: Fenton, electro-Fenton, and photo-Fenton. Journal of Hazardous Materials **154:**655-662.
29. **Sun N, Parthasarathi R, Socha AM, Shi J, Zhang S, Stavila V, Sale KL, Simmons BA, Singh S.** 2014. Understanding pretreatment efficacy of four cholinium and imidazolium ionic liquids by chemistry and computation. Green Chemistry **16:**2546-2557.
30. **Salvachúa D, Katahira R, Cleveland NS, Khanna P, Resch MG, Black BA, Purvine SO, Zink EM, Prieto A, Martínez MJ, Simmons BA, Gladden JM, Beckham GT.** 2016. Lignin depolymerization by fungal secretomes and a microbial sink. Green Chemistry **18:**6046-6062.
31. **Kent MS, Avina IC, Rader N, Busse ML, George A, Sathitsuksanoh N, Baidoo EEK, Timlin JA, Giron NH, Celina MC, Martin LE, Polsky R, Chavez VH, Huber DL, Keasling JD, Singh S, Simmons BA, Sale KL.** 2015. Assay for lignin breakdown based on lignin films: insights into the Fenton reaction with insoluble lignin. Green Chemistry **17:**4830-4845.
32. **Contreras DF, J.; Rodriguez, J.** 2006. Veratryl alcohol degredation by a catechol-driven Fenton reaction as lignin oxidation by brown-rot fungi model. International Biodeterioration & Biodegradation **57:**63-68.
33. **Contreras DR, J.; Freer, J.; Schwederski, B.; Kaim, W.** 2007. Enhanced hydroxyl radical production by dihydroxybenzene-driven Fenton reactions: implications for wood biodegradation. J Biol Inorg Chem **12:**1055-1061.
34. **Rodriguez JC, D.; Oviedo, O.; Freer, J.; Baeza, J.** 2004. Degradation of recalcitrant compounds by catechol-driven Fenton reaction. Water Science and Technology **49:**81-84.
35. **Salgado P, Melin V, Duran Y, Mansilla H, Contreras D.** 2017. The reactivity and reactiono pathway of fenton reactions driven by substituted 1,2-dihydroxybenzenes. Environmental Science & Technology **51:**3687-3693.
36. **Melin V, Henriquez A, Radojkovic C, Schwederski B, Kaim W, Freer J, Contreras D.** 2016. Reduction reactivity of catecholamines and their ability to promote a Fenton reaction. Inorganic Chimica Acta **453:**1-7.
37. **Charkoudian LK, Franz KJ.** 2006. Fe(III)-coordination properties of neuromelanin components: 5,6-dihydroxyindole and 5,6-dihydroxylindole-2-carboxylic acid. Inorganic Chemisty **45:**3657-3664.
38. **Hammel KE, Kapich AN, Jensen J, K. A., Ryan ZC.** 2002. Reactive oxygen species as agents of wood decay by fungi. Enzyme and Microbial Technology **30:**445-453.
39. **Zeng J, Yoo CG, Wang F, Pan X, Vermerris W, Tong Z.** 2015. Biomimetic Fenton-catalysed lignin depolymerization to high-value aromatics and dicarboxylic acids. ChemSusChem **8:**861-871.
40. **Hilden L, Johansson G, Pettersson G, Li J, Ljungquist P, Henriksson G.** 2000. Do the extracellular enzymes cellobiose dehydrogenase and manganese peroxidase form a pathway in lignin biodegradation? FEBS Lett **477:**79-83.
41. **Hu G, Cateto C, Pu Y, Samuel R, Ragauskas AJ.** 2011. Structural characterization of switchgrass lignin after ethanol organosolv pretreatment. Energy & Fuels **26:**740-745.
42. **Faix O.** 1991. Classification of lignins from different botanical origins by FT-IR spectroscopy. Holzforschung **45:**21-27.
43. **Boeriu C, Bravo D, Gosselink RJA, van Dam JEG.** 2004. Characterization of structure-dependent functional properties of lignin with infrared spectroscopy. Industrial Crops and Products **20:**205-218.
44. **Zhou G, Taylor G, Polle A.** 2011. FTIR-ATR-based prediction and modelling of lignin and energy contents reveals independent intra-specific variation of these traits in bioenergy poplars. Plant Methods **7:**9.
45. **Gordobil O, Moriana R, Zhang L, Labidi J, O. S.** 2016. Assesment of technical lignins for uses in biofuels and biomaterials: Structure-related properties, proximate analysis and chemical modification. Industrial Crops and Products **83:**155-165.
46. **Katrizky AR, Coats NA.** 1959. Infrared absorption of substituents in aromatic systemes. Part I. Methoxy- and ethoxy- compounds. Journal of the Chemical Society **0:**2062-2066.
47. **Mancera A, Fierro V, Pizzi A, Dumarçay S, Gérardin P, Velásquez J, Quintana G, Celzard A.** 2010. Physicochemical characterization of sugar cane bagasse lignin oxidized by hydrogen peroxide. Polymer Degradation and Stability **95:**470-476.
48. **El-Nemr KF, Mohamed RM.** 2017. Sorbic acid as friendly curing agent for enhanced properties of ethylene propylene diene monomer rubber using gamma radiation. Journal of Macromolecular Science, Part A **54:**711-719.
49. **Max J-J, Chapados C.** 2002. Infrared spectroscopy of aqueous carboxylic acids: malic acid. J Phys Chem A **106:**6452-6461.
50. **Wagner CC, Baran EJ.** 2010. Vibrational spectra of two Fe(III)/EDTA complexes useful for iron supplementation. Spectrochimica Acta Part A: Molecular and Biomolecular Spectroscopy **75:**807-810.
51. **He W, Gao W, Fatehi P.** 2017. Oxidation of kraft lignin with hydrogen peroxide and its application as a dispersant for kaolin suspensions. ACS Sustainable Chem Eng **5:**10597-10605.
52. **Areskogh D, Li J, Gellerstedt G, Henricksson G.** 2010. Investigation of the molecular weight increase of commercial lignosulfonates by laccase catalysis. Biomacromolecules **11:**904-910.
53. **Areskogh D, Henriksson G.** 2011. Fenton's reaction: a simple and versatile method to structurally modify commercial lignosulphonates. Nordic Pulp and Paper Research Journal **26:**90-98.
54. **Mohanty S, Das B, Dhara S.** 2013. Poly(maleic acid) - A novel dispersant for aqueous alumina slurry. Journal of Asian Ceramic Societies **1:**184-190.
55. **Tadros T.** 2009. Polymeric surfactants in disperse systems. Advances in Colloid and Interface Science **147-148:**281-299.
56. **Sahimi M.** 1994. Applications of Percolation Theory. Taylor & Francis, Bristol, PA.

57. **Qin YY, L.; Wu, R.; Yang, D.; Qiu, X.; Zhu, J. Y.** 2016. Biorefinery Lignosulfonates from Sulfite-Pretreated Softwoods as Dispersant for Graphite. ACS Sustainable Chemistry and Engineering **4:**2200-2205.
58. **Aro T, Fatehi P.** 2017. Production and application of lignosulfonates and sulfonated lignin. ChemSusChem **10:**1861-1877.
59. **Ansari A, Pawlik M.** 2007. Floatability of chalcopyrite and molybdenite in the presence of lignosulfonates. Part I. Adsorption studies. Minerals Engineering **20:**600-608.
60. **Huber D, Ortner A, Daxbacher A, Nyanhongo GS, Bauer W, Guebitz GM.** 2016. Influence of oxygen and mediators on laccase-catalyzed polymerization of lignosulfonate. ACS Sustainable Chemistry & Engineering **4:**5303-5310.
61. **Kjellander M, Gotz K, Liljeruhm J, Boman M, Johansson G.** 2013. Steady-state generation of hydrogen peroxide: kinetics and stability of alcohol oxidase immobilized on nanoporous alumina. Biotechnol Lett **35:**585-590.
62. **Lopez C, Cavaco-Paulo A.** 2008. In-situ enzymatic generation of hydrogen peroxide for bleaching purposes. Eng Life Sci **8:**315-323.
63. **Kremer SM, Wood PM.** 1992. Production of Fenton's reagent by cellobiose oxidase from cellulolytic cultures of *Phanerochaete chrysosporium*. Eur J Biochem **208:**807-814.

1